Cooperative Guidance Law for Target Pair to Lure Two Pursuers into Collision

Zheng Wen Tan*, Robert Fonod† and Tal Shima‡

Technion - Israel Institute of Technology, Haifa 3200003, Israel

A novel cooperative defensive guidance law is presented for a two-on-two engagement. Instead of classical strategies in which evasive maneuvers are performed or additional agents (e.g., defender missiles) are deployed, the target pair lures the pursuing missiles into collision. The optimal cooperative strategy is solved using state-dependent Riccati equation method. Linearized kinematics and arbitrary-order linear adversaries' dynamics are assumed in the guidance law derivation. Imperfect information is assumed on the relative states and the guidance laws employed by the missile pair. Guidance strategies that the pursuing missiles may employ are assumed to belong to a finite set of linear guidance laws. In addition to the proposed cooperative defensive strategy, a decentralized estimation scheme based on the multiple-model adaptive estimation approach is also presented. Guidance law and estimation performance are demonstrated using nonlinear simulations. Simulation results show the viability of the proposed guidance law and highlight the sensitivity of the guidance law to range measurement accuracy.

*Graduate Student, Department of Aerospace Engineering, zheng-wen@campus.technion.ac.il.
†Postdoctoral Fellow, Department of Aerospace Engineering, robert.fonod@technion.ac.il.
‡Professor, Department of Aerospace Engineering, tal.shima@technion.ac.il. Associate Fellow AIAA.

Nomenclature

$\boldsymbol{A}$, $\boldsymbol{B}$, $\boldsymbol{C}$	=	linearized collision geometry state-space model matrices
$\boldsymbol{A}_v$, $\boldsymbol{B}_v$, $\boldsymbol{C}_v$, d_v	=	state-space model matrices of the dynamics of vehicle v
a	=	acceleration normal to flight path angle
c	=	center of the line-of-sight between missiles
g	=	gravitational constant
$\boldsymbol{H}$	=	measurement matrix
$\boldsymbol{K}_{MTi}$	=	gain matrix for linear guidance law
J	=	cost function
$\mathbb{N}$	=	set of natural numbers
$\mathcal{N}$	=	normal distribution
N'	=	missile guidance gain
$\boldsymbol{P}_{MTi}$	=	covariance matrix of the ith estimator
$\boldsymbol{P}$	=	matrix solution to the Riccati equation
$\boldsymbol{Q}$	=	matrix of weights on states in running cost
$\boldsymbol{Q}_f$	=	matrix of weights on states in terminal cost
$\mathbb{R}^n$	=	set of real numbers of dimension n
$\boldsymbol{R}_{MTi}$	=	noise covariance matrix of measurements of the ith estimator
$\boldsymbol{R}$	=	matrix of weights on targets' control effort
$\boldsymbol{S}_i^j$	=	covariance matrix of the jth regime-matched filter of the ith estimator
T_s	=	sampling period
t	=	time
t_f	=	final time
$\mathcal{U}_i$	=	set of possible guidance laws considered in the estimator of ith target
$\mathcal{U}_{comb}$	=	set of possible combination of guidance laws considered
$\boldsymbol{u}$	=	control vector of vehicle group
u	=	control input of vehicle
V	=	speed
V_C	=	closing speed
$\boldsymbol{v}$	=	measurement noise
X_c^0, Y_c^0	=	initial position coordinates of c

$\bar{X}_c^0$, $\bar{Y}_c^0$	=	normalized X_c^0, Y_c^0
X_I, Y_I	=	inertial position coordinates
$\boldsymbol{x}$	=	state vector for estimation purposes
$\boldsymbol{x}_v$	=	state vector representing the dynamics of vehicle v
$\boldsymbol{y}$	=	linear system state vector
$\boldsymbol{y}_v$	=	component of $\boldsymbol{x}_v$ orthogonal to the associated line-of-sight
y	=	relative displacement normal to initial line-of-sight
$\boldsymbol{Z}_i(0)$	=	a priori information of the missile by the ith target
$\boldsymbol{z}_i$	=	measurement vector of the ith target
γ	=	flight-path angle
Δ	=	time difference between time to missile-missile collision and missile-target collision
δ, θ	=	angles between the velocity vector and line-of-sight of the pursuer and target respectively
Λ_i^j	=	jth mode-conditioned likelihood function of the ith estimator
λ	=	line-of-sight angle
μ_i^j	=	jth regime probability for the ith estimator
$\boldsymbol{\nu}_i^j$	=	innovations vector of the jth regime-matched filter of the ith estimator
ξ_{MT}	=	normalized time
ρ	=	range
$\bar{\rho}_{MM}^0$	=	normalized ρ_{MM}^0
$\sigma_{i,\rho}^2$, $\sigma_{i,\lambda}^2$	=	range and line-of-sight angle measurement noise variances of the ith estimator respectively
τ_v	=	first-order lag of vehicle v

Subscripts

Mi	=	ith missile
MM	=	missile versus missile engagement
MTi	=	ith missile versus ith target engagement
Ti	=	ith target
v	=	vehicle

Superscripts

lin	=	linear
max	=	maximum
NL	=	nonlinear
0	=	initial condition
*	=	optimal

I. Introduction

Multi-vehicle cooperation has received much attention in recent years as it has shown tremendous potential in missions such as wide area persistent surveillance [1], cooperative tactical reconnaissance [2], and cooperative salvo attack [3]. While guidance strategies have been developed specifically for the aforementioned missions, limited work has been done to study how cooperation could improve the survivability of such multi-vehicle teams. This becomes increasingly important as counter measures, for example in [4], are developed to take down such teams before they could complete their missions. In this paper, the problem of aircraft survivability in a multi-vehicle engagement is tackled. Specifically, a cooperative defensive strategy is derived for a pair of aircraft (henceforth known as "targets" and abbreviated as "T") being pursued by a pair of missiles (henceforth known interchangeably as "missiles" or "pursuers" and abbreviated as "M").

The classical approach from a target's perspective in a missile-target engagement is to maximize the miss distance between itself and the missile. Research on optimal target evasion strategies in a 1-on-1 scenario has been well-established. Optimal evasion strategies have been solved using two approaches: 1) by formulating the problem as a pursuit-evasion differential game [5–8], or 2) a one-sided optimal evasion problem. In the latter, the missile guidance strategy is assumed to be known to the target [9–13]. The works in [9–12] studied the optimal evasion problem against a missile using proportional navigation (PN) while in [13], optimal evasion strategies were also solved for missiles using augmented PN (APN) and optimal guidance law (OGL).

A key assumption in a one-sided optimal evasion problem is that the target must have exact knowledge of the missile's guidance strategy. Works such as [14, 15] relaxed this assumption by incorporating a multiple-model-adaptive-estimator (MMAE) to identify the guidance law of the pursuing missile. First pioneered by Magill [16], the MMAE approach is applied on a one-sided optimal evasion problem in [15] where it was assumed that the pursuing missile is employing one of a finite set of linear guidance laws and guidance parameters. Known often as a "mode" or "regime", each model in the MMAE represents a

possible missile guidance law and its corresponding guidance parameter. During the estimation process, the MMAE scheme runs a bank of filters (such as the extended Kalman Filter (EKF) used in [15]) in parallel with a filter matching each of the possible regimes. Estimation of the system states is obtained by a weighted sum of the state estimates from each filter in the bank and the weights represent the probability of each regime matching the true guidance strategy of the pursuing missile based on measurement history. Regime probabilities are updated at each time step using Bayesian inference. It is calculated based on the previous time step's regime probabilities and the regime-conditioned likelihood of the new measurement. One-sided optimal evasion is solved for each of the possible regimes and the final target maneuver is derived under a multiple model adaptive control (MMAC) [17] framework. In the MMAC approach, the final evasion command is determined by either the minimum mean square error (MMSE) criterion where the command is a regime probability weighted sum of every optimal maneuver matched to each possible regime, or a maximum a posteriori probability (MAP) criterion where the latter matches the optimal maneuver against the regime that is most likely to be true.

An alternative target defensive strategy aside from purely evading is to use defender missiles to intercept the pursuer[13, 14, 18, 19]. This strategy is especially advantageous for a target that has large maneuverability disadvantage over its pursuer and pursuer-target interception is unavoidable using purely evasive maneuvers. Shaferman and Shima [14] developed a multiple-model adaptive guidance strategy to the three-body problem in which a MMAE is applied to identify the pursuer's guidance strategy so that the target-defender team could maneuver optimally to enforce pursuer-defender interception. Besides solving this three-body engagement as a one-sided optimal control problem, different approaches were also proposed by works such as [18, 19]. Ratnoo and Shima [18] derived a guidance strategy in which the defender employs line-of-sight (LOS) guidance to maintain its position on the LOS connecting the target platform to the pursuer. Kumar and Shima [19] developed nonlinear guidance strategies based on sliding-mode control techniques and highlighted its effectiveness even if there were large errors in the initial heading and the time-to-go estimates for the defender.

In this paper, we consider the problem of a 2-on-2 scenario in which the objective of the target pair is to survive the engagement by luring the two pursuers into collision with each other through cooperative maneuvers. This problem, to the best of the authors' knowledge, has not been explored in open literature. It differs from previous works as the target pair does not simply evade from their pursuers nor do they require additional defender missiles to survive the engagement. The proposed strategy does, however, draw inspiration from the target-defender-pursuer engagement but instead of luring the pursuers into a defender, the targets capitalize on the presence of multiple adversaries to guide the pursuers into collision

with themselves. This multiple-missile engagement also presents an interesting challenge when incorporating the MMAE with the cooperative guidance strategy as the latter is unique to each possible combination of guidance laws employed by the missile pair. If the MMAE problem is solved conventionally, in which each possible combination is modeled by a separate filter in the regime bank, the number of filters will grow quadratically with the number of possible missile guidance laws considered for each missile and can become computationally intensive.

The main contribution of this paper is to present a novel cooperative defensive strategy for the target pair in a 2-on-2 scenario in which the targets ensure their survivability by luring the pursuing missiles into collision. It is assumed that the pursuers' are using one of the finite set of linear guidance laws. The target pair is assumed to know this set but not the active guidance laws being employed by the missiles. The vehicles are assumed to have arbitrary-order linear dynamics. In addition, a decentralized MMAE approach is proposed for state estimation and missile guidance law identification. In this decoupled approach, each target only computes the estimates of states related to its own pursuer and need not account explicitly every possible guidance law combination of the pursuer pair in its regime bank. While the target pair has imperfect information of the relative states between the missiles and the targets, perfect information of the targets' positions, accelerations, and flight path angles are assumed. Communication of the above information between the targets is also assumed to occur with zero lag.

The remainder of this paper is organized as follows. Description of the 2-on-2 engagement and its mathematical model will be presented in Section II. Subsequently the cooperative optimal guidance law of the target pair is derived in Section III and the MMAC-based cooperative guidance strategy is presented in Section IV. Detailed analysis of the performance is shown in Section V. Finally, some concluding remarks will be made in Section VI.

II. Engagement Formulation

Consider a scenario with 2 missiles homing on 2 targets. The objective of the targets in this engagement is to conduct cooperative guidance so that the pursuers are lured into interception with each other without any of the targets being intercepted by the missiles. In addition, we assume the problem can be simplified to a point-mass, planar engagement, and effects of gravity can be neglected. All vehicles use skid-to-turn control with roll-stabilization. All vehicles are assumed to have constant speeds and perform lateral maneuvers only. Imperfect information on the relative states between each missile and target is assumed while perfect information on those between the targets is considered. Lag-free communication of all states between the targets are also assumed. Each target in the engagement is assumed

to be pursued by one missile, and each missile pursues only one target. The missile pair is also assumed to have no knowledge that they are on a collision course with each other.

Schematic of the engagement can be seen in Figure 1, where $X_I - O_I - Y_I$ denotes the Cartesian, inertial reference frame.

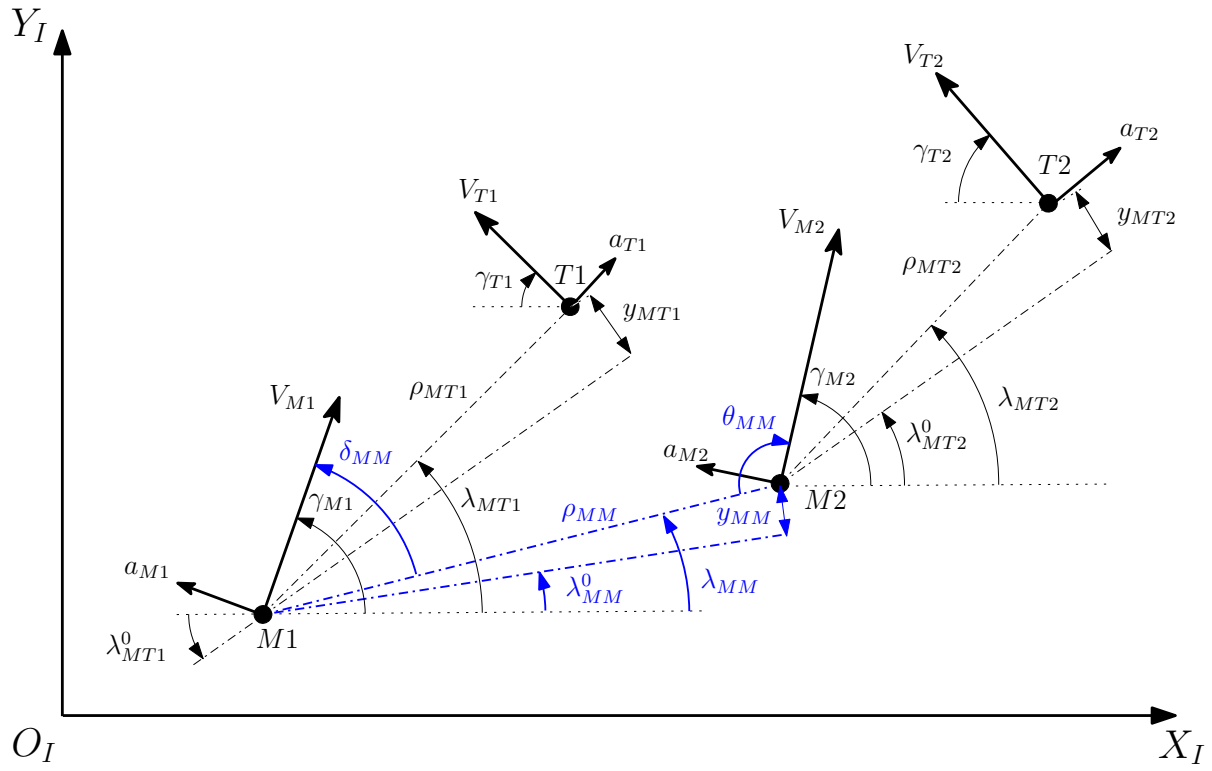

Figure 1: Schematic of a 2-on-2 Engagement.

II.A. Nonlinear Kinematics

Consider first the kinematics of the Mi–Ti engagement, $i \in \{1, 2\}$, in the 2-on-2 scenario (Figure 1). Defining the latter in polar coordinates $(\rho_{MTi}, \lambda_{MTi})$ referenced to Mi, Ti's state vector of Mi is

$$\boldsymbol{x}_{MTi} = \begin{bmatrix} \rho_{MTi} & \lambda_{MTi} & \boldsymbol{x}_{Mi} & \gamma_{Mi} & V_{Mi} \end{bmatrix}^T \tag{1}$$

where $\boldsymbol{x}_{Mi}$ is the internal state vector of Mi associated with its dynamics. Assuming the velocity of each vehicle $v \in \{Mi, Ti\}$ is constant near the endgame and their dynamics can be represented by an arbitrary-order linear system, i.e.,

$$\left.\begin{aligned} \dot{\boldsymbol{x}}_v &= \boldsymbol{A}_v \boldsymbol{x}_v + \boldsymbol{B}_v u_v \\ a_v &= \boldsymbol{C}_v \boldsymbol{x}_v + d_v u_v \end{aligned}\right\} \tag{2}$$

the equations of motion (EOM) associated with $\boldsymbol{x}_{MTi}$ are:

$$\left.\begin{array}{rcl} \dot{\rho}_{MTi} & = & -V_{C,MTi} \\ \dot{\lambda}_{MTi} & = & V_{\lambda,MTi}/\rho_{MTi} \\ \dot{\boldsymbol{x}}_{Mi} & = & \boldsymbol{A}_{Mi}\boldsymbol{x}_{Mi} + \boldsymbol{B}_{Mi}u_{Mi} \\ \dot{\gamma}_{Mi} & = & a_{Mi}/V_{Mi} \\ \dot{V}_{Mi} & = & 0 \end{array}\right\} \tag{3}$$

where the closing speed of the Mi–Ti engagement, $V_{C,MTi}$ is

$$V_{C,MTi} = V_{Ti}\cos(\gamma_{Ti} + \lambda_{MTi}) + V_{Mi}\cos(\gamma_{Mi} - \lambda_{MTi}) \tag{4}$$

the speed orthogonal to the Mi–Ti LOS, $V_{\lambda,MTi}$, is

$$V_{\lambda,MTi} = V_{Ti}\sin(\gamma_{Ti} + \lambda_{MTi}) - V_{Mi}\sin(\gamma_{Mi} - \lambda_{MTi}) \tag{5}$$

and γ_{Ti} is defined by the following:

$$\dot{\gamma}_{Ti} \;=\; a_{Ti}/V_{Ti} \tag{6}$$

where a_{Ti} is defined in (2).

In addition to kinematics between the missiles and targets, the relative motion between $M1$ and $M2$ is also described in a similar manner as (3), i.e.,

$$\left.\begin{array}{rcl} \dot{\rho}_{MM} & = & -V_{C,MM} \\ \dot{\lambda}_{MM} & = & V_{\lambda,MM}/\rho_{MM} \end{array}\right\} \tag{7}$$

where

$$V_{C,MM} = -V_{M2}\cos(\gamma_{M2} - \lambda_{MM}) + V_{M1}\cos(\gamma_{M1} - \lambda_{MM}) \tag{8}$$

$$V_{\lambda,MM} = V_{M2}\sin(\gamma_{M2} - \lambda_{MM}) - V_{M1}\sin(\gamma_{M1} - \lambda_{MM}) \tag{9}$$

II.B. Measurement Model

It is assumed that the targets are using electro-optic seekers and/ or radars to acquire measurements. Therefore, each target may either measure ρ_{MTi} and λ_{MTi} or only λ_{MTi}, where $i \in \{1, 2\}$. The discrete time measurements, $\boldsymbol{z}_{MTi}(k) \in \mathbb{R}^{n_z}$, are corrupted by a zero-mean, mutually independent, white Gaussian measurement noise, $\boldsymbol{v}_{MTi}(k) \in \mathbb{R}^{n_z}$. Therefore,

the measurement model of the ith estimator, when both ρ_{MTi} and λ_{MTi} are available, is

$$\boldsymbol{z}_{MTi}(k) = \boldsymbol{H}\boldsymbol{x}_{MTi}(k) + \boldsymbol{v}_{MTi}(k) = \begin{bmatrix} \rho_{MTi}(k) \\ \lambda_{MTi}(k) \end{bmatrix} + \boldsymbol{v}_{MTi}(k) \tag{10}$$

where

$$\boldsymbol{v}_{MTi}(k) \sim \mathcal{N}([0]_{n_z \times 1}, \boldsymbol{R}_{MTi})), \quad \boldsymbol{R}_{MTi} = \text{diag}(\sigma^2_{i,\rho}, \sigma^2_{i,\lambda}) \tag{11}$$

such that $\boldsymbol{H}$ is the corresponding measurement matrix and $\boldsymbol{R}_{MTi}$ is the covariance matrix with $\sigma^2_{i,\rho}$ and $\sigma^2_{i,\lambda}$ being the variances for the range and LOS angle measurements acquired by ith target respectively. In the case when only λ_{MTi} is acquired, the first row of $\boldsymbol{H}$ is removed and $R_{MTi} = \sigma^2_{i,\lambda}$.

III. Optimal Cooperative Guidance Law for the Target Pair

In this section, the optimal cooperative guidance law for the target pair is derived. The optimal strategy is solved using linearized kinematics. It is assumed that the missiles are using a linear guidance law that is known to the target pair through an identification scheme such as the one that will be presented in Section IV.A.

III.A. Linearized Kinematics for Guidance Law Derivation

Classical linearization [11] about the collision triangles in the engagement is performed with reference to each triangle's initial LOS. The state y_{MTi}, $i \in \{1, 2\}$ is defined as the separation between Mi and Ti orthogonal to the initial LOS of Mi and Ti while y_{MM} is the separation between $M1$ and $M2$ orthogonal to the initial LOS of $M1$ and $M2$ (Figure 1).

Since the objective for the target pair defined in this paper is to survive the engagement by cooperatively luring the missiles into collision, the guidance law should drive the final time of the $M1-M2$ engagement, $t_{f,MM}$, to occur earlier than both $M1-T1$ and $M2-T2$ engagements, i.e.,

$$t_{f,MM} < \min(t_{f,MT1}, t_{f,MT2}) \tag{12}$$

However, depending on initial positions and flight path angles of the missiles, condition (12) need not necessarily hold. Referring to Figure 1, it is evident that in order to reduce $t_{f,MM}$, the target pair should minimize the magnitude of δ_{MM} and θ_{MM} so as to increase the closing velocity of the $M1-M2$ engagement. To this end, the linearized model is formulated

incorporating the latter two states.

Thus, to solve for the optimal guidance law, the following linearized state vector $\boldsymbol{y}$ is defined:

$$\boldsymbol{y} = \begin{bmatrix} \boldsymbol{y}_{MT1}^T & \boldsymbol{y}_{MT2}^T & \boldsymbol{y}_{MM}^T & \delta_{MM} & \theta_{MM} \end{bmatrix}^T \tag{13}$$

where

$$\boldsymbol{y}_{MM} = \begin{bmatrix} y_{MM} & \dot{y}_{MM} \end{bmatrix}^T, \quad \boldsymbol{y}_{MTi} = \begin{bmatrix} y_{MTi} & \dot{y}_{MTi} & \boldsymbol{y}_{Mi}^T & \boldsymbol{y}_{Ti}^T \end{bmatrix}^T, \quad i \in \{1, 2\} \tag{14}$$

The internal state vectors $\boldsymbol{y}_{Mi}$ and $\boldsymbol{y}_{Ti}$ are the components of the $\boldsymbol{x}_{Mi}$ and $\boldsymbol{x}_{Ti}$ orthogonal to the initial line-of-sight of the $Mi - Ti$ engagement and

$$\left.\begin{array}{rcl} \delta_{MM} & \triangleq & \gamma_{M1} - \lambda_{MM} \\ \theta_{MM} & \triangleq & \pi - (\gamma_{M2} - \lambda_{MM}) \end{array}\right\} \tag{15}$$

The linearized EOM are:

$$\dot{\boldsymbol{y}} = \begin{cases} \dot{y}_1 & = & y_2 \\ \dot{y}_2 & = & a_{T1}^{\perp} - a_{M1}^{\perp} \\ \dot{\boldsymbol{y}}_{M1} & = & \boldsymbol{A}_{M1}\boldsymbol{y}_{M1} + \boldsymbol{B}_{M1}u_{M1}^{\perp} \\ \dot{\boldsymbol{y}}_{T1} & = & \boldsymbol{A}_{T1}\boldsymbol{y}_{T1} + \boldsymbol{B}_{T1}u_{T1}^{\perp} \\ \dot{y}_{n_{MT1}+3} & = & y_{n_{MT1}+4} \\ \dot{y}_{n_{MT1}+4} & = & a_{T2}^{\perp} - a_{M2}^{\perp} \\ \dot{\boldsymbol{y}}_{M2} & = & \boldsymbol{A}_{M2}\boldsymbol{y}_{M2} + \boldsymbol{B}_{M2}u_{M2}^{\perp} \\ \dot{\boldsymbol{y}}_{T2} & = & \boldsymbol{A}_{T2}\boldsymbol{y}_{T2} + \boldsymbol{B}_{T2}u_{T2}^{\perp} \\ \dot{y}_{n_{MT1}+n_{MT2}+5} & = & y_{n_{MT1}+n_{MT2}+6} \\ \dot{y}_{n_{MT1}+n_{MT2}+6} & = & -a_{M2}^{\perp}C_{MM}^{\theta}/C_{MT2}^{\delta} - a_{M1}^{\perp}C_{MM}^{\delta}/C_{MT1}^{\delta} \\ \dot{y}_{n_{MT1}+n_{MT2}+7} & = & \dot{\gamma}_{M1} - \dot{\lambda}_{MM} \\ \dot{y}_{n_{MT1}+n_{MT2}+8} & = & \dot{\lambda}_{MM} - \dot{\gamma}_{M2} \end{cases} \tag{16}$$

where for $i \in \{1, 2\}$, $n_{Mi} = \dim(\boldsymbol{A}_{Mi})$, $n_{Ti} = \dim(\boldsymbol{A}_{Ti})$ and

$$n_{MTi} = n_{Mi} + n_{Ti} \tag{17}$$

and for $E \in \{MT1, MT2, MM\}$, $\eta \in \{\delta, \theta\}$

$$C_E^\eta = \cos \eta_E \tag{18}$$

with δ_{MTi} and θ_{MTi} defined as

$$\left.\begin{aligned} \delta_{MTi} &= \gamma_{Mi} - \lambda_{MTi} \\ \theta_{MTi} &= \gamma_{Ti} + \lambda_{MTi} \end{aligned}\right\} \tag{19}$$

and δ_{MM} and θ_{MM} as presented in (15).

In (16), the superscript $\perp$ represents the component of the acceleration orthogonal to the associated LOS, i.e., for $i \in \{1, 2\}$

$$a_{Ti}^\perp = a_{Ti} C_{MTi}^\theta \tag{20}$$

$$a_{Mi}^\perp = a_{Mi} C_{MTi}^\delta \tag{21}$$

Assuming linearization holds, $\dot{\lambda}_{MM}$ defined in (7) is incorporated into (16) in its linearized form as:

$$\dot{\lambda}_{MM} = \frac{y_{MM} + \dot{y}_{MM} t_{go,MM}}{V_{C,MM} t_{go,MM}^2} \tag{22}$$

where $V_{C,MM}$ is defined in (8) and $t_{go,MM}$ is defined as

$$t_{go,MM} = t_{f,MM} - t \tag{23}$$

Next, the missiles are assumed to be using a linear guidance law in the following form:

$$u_{Mi}^\perp = \boldsymbol{K}_{MTi} \boldsymbol{y}_{MTi} + K_{u_{Ti}} u_{Ti}^\perp \tag{24}$$

where

$$\boldsymbol{K}_{MTi} = \begin{bmatrix} K_1^{Mi} & K_2^{Mi} & \boldsymbol{K}_{Mi} & \boldsymbol{K}_{Ti} \end{bmatrix}, \quad i \in \{1, 2\} \tag{25}$$

Remark 1 *In this paper, the cooperative guidance law is derived against missiles using PN* [20]*, APN* [21] *and OGL* [22]*. For the sake of brevity, gains of these well-established linear guidance laws,* $\boldsymbol{K}_{MTi}$ *and* $K_{u_{Ti}}$ *are not explicitly defined in this paper. Readers are referred to [15] for the detailed formulation of these guidance laws.*

Assuming that information about $\boldsymbol{K}_{MTi}$ and $K_{u_{Ti}}$ is known to the target group, (16) can be formulated as a one-sided optimal control problem, i.e:

$$\dot{\boldsymbol{y}} = \boldsymbol{A}(t)\boldsymbol{y}(t) + \boldsymbol{B}(t)\boldsymbol{u}_T(t) \tag{26}$$

such that

$$\boldsymbol{A}(t) = \begin{bmatrix} \boldsymbol{A}_{MT1} & [0] & [0] \\ [0] & \boldsymbol{A}_{MT2} & [0] \\ \boldsymbol{A}_{MM}^{M1} & \boldsymbol{A}_{MM}^{M2} & \boldsymbol{A}_{MM}^{0} \end{bmatrix}, \quad \boldsymbol{B}(t) = \begin{bmatrix} \boldsymbol{B}_{MT1} & [0] \\ [0] & \boldsymbol{B}_{MT2} \\ \boldsymbol{B}_{MM}^{T1} & \boldsymbol{B}_{MM}^{T2} \end{bmatrix},$$
$$\boldsymbol{u}_T(t) = \begin{bmatrix} u_{T1}^{\perp} & u_{T2}^{\perp} \end{bmatrix}^T \tag{27}$$

where [0] is a matrix of zeros with appropriate dimensions. Elements of $\boldsymbol{A}(t)$ and $\boldsymbol{B}(t)$ are defined in Appendix A.

III.B. Optimal Cooperative Guidance Law Derivation

As discussed above, (12) may not hold for all initial conditions. Thus, in order to derive a guidance law that can drive the system towards achieving (12), states δ_{MM} and θ_{MM} need to be incorporated into the cost function of the optimal control problem.

The cost is defined using the finite horizon, linear-quadratic formulation:

$$J = \boldsymbol{y}^T(t_{f,MM})\boldsymbol{Q}_f\boldsymbol{y}(t_{f,MM}) + \int_{t_0}^{t_{f,MM}} \left[\boldsymbol{y}^T(t)\boldsymbol{Q}\boldsymbol{y}(t) + \boldsymbol{u}_T^T(t)\boldsymbol{R}\boldsymbol{u}_T(t)\right] dt \tag{28}$$

where

$$\boldsymbol{Q}_f = \begin{bmatrix} [0] & [0] \\ [0] & \boldsymbol{w_f} \end{bmatrix}, \qquad \boldsymbol{w_f} = \begin{bmatrix} w_{ms} & [0] \\ [0] & [0] \end{bmatrix}$$
$$\boldsymbol{Q} = \begin{bmatrix} [0] & [0] \\ [0] & \boldsymbol{w_r} \end{bmatrix}, \qquad \boldsymbol{w_r} = \begin{bmatrix} w_\delta & 0 \\ 0 & w_\theta \end{bmatrix} \tag{29}$$
$$\boldsymbol{R} = \begin{bmatrix} w_{u1} & 0 \\ 0 & w_{u2} \end{bmatrix}$$

The weights in (29) are defined as follows: w_{ms} is the weight on $y_{MM}(t_{f,MM})$; w_δ and w_θ are weights on the angles δ_{MM} and θ_{MM} that were defined in (15) and shown in Figure 1; w_{u1} and w_{u2} are weights on $u_{T1}^{\perp}$ and $u_{T2}^{\perp}$ respectively.

The objective of the optimal controller, $\boldsymbol{u}_T^*(t)$, is to minimize J in (28), i.e.,

$$\boldsymbol{u}_T^*(t) = \arg\min_{\boldsymbol{u}_T \in \Omega} J \tag{30}$$

where Ω is the set of admissible controls.

Solution to the problem defined in (30) is given by:

$$\boldsymbol{u}_T^*(t) = -\boldsymbol{R}^{-1}\boldsymbol{B}^T(t)\boldsymbol{P}(t)\boldsymbol{y}(t) \tag{31}$$

where $\boldsymbol{P}(t)$ is the solution to the differential Riccati equation [23]:

$$-\dot{\boldsymbol{P}}(t) = \boldsymbol{P}(t)\boldsymbol{A}(t) + \boldsymbol{A}^T(t)\boldsymbol{P}(t) - \boldsymbol{P}(t)\boldsymbol{B}\boldsymbol{R}^{-1}\boldsymbol{B}^T\boldsymbol{P}(t) + \boldsymbol{Q}(t), \quad \boldsymbol{P}(t_f) = \boldsymbol{Q}_f \tag{32}$$

Physically, $\boldsymbol{u}_T^*(t)$ not only minimizes the miss distance between the missiles at $t_{f,MM}$ with minimal control effort, it also minimizes the weighted sum of δ_{MM}^2 and θ_{MM}^2 over $[t_0, t_{f,MM}]$ to maximize $V_{C,MM}$ and drive the missiles to collision before they could hit the targets. Note that this is unlike classical linearization assumptions for missile-target engagements [11] where the geometry of the collision triangle is assumed to be near constant since $\boldsymbol{u}_T^*$ is altering the collision geometry at each time step by minimizing δ_{MM}^2 and θ_{MM}^2.

III.C. Implementing the Linear Optimal Strategy in the Nonlinear Engagement

The optimal controller, $\boldsymbol{u}_T^*$, in (31) is solved in the linearized frame and represents the required control that is orthogonal to corresponding line-of-sight. This subsection describes how $\boldsymbol{u}_T^*$ is implemented in the proposed guidance strategy to obtain the nonlinear controller $\boldsymbol{u}_T^{NL}$.

As noted in Section III.B, in such 2-on-2 engagements there exist initial conditions in which the missiles are not on the required collision triangle such that condition (12) is met. In such conditions, the targets are required to maneuver in a way such that the initial collision geometry is altered to meet condition (12). Thus, the classical linearization assumption of the collision geometry remaining constant is no longer valid and in order to implement the proposed linear controller, this paper employs the State Dependent Riccati Equations (SDRE) method [24]. Under the SDRE framework, the nonlinear engagement is re-linearized at every time step k and (32) is solved online to obtain $\boldsymbol{u}_T^*(k)$. Finally, in order to obtain the required nonlinear control at each time step, $\boldsymbol{u}_T^{NL}(k)$, $\boldsymbol{u}_T^*(k)$ is resolved to the direction orthogonal to the target's velocity vector, i.e.,

$$u_{Ti}^{NL}(k) = \frac{u_{Ti}^*(k)}{\cos[\gamma_{Ti}(k) + \lambda_{MTi}(k)]}, \quad i \in \{1, 2\} \tag{33}$$

In order to solve for $\boldsymbol{u}_T^*$, integration of (32) from $t_{go,MM} \in [0, t_{f,MM}]$ is required. Since it is assumed that the missile is using classical missile guidance laws, there exist elements that are inversely proportional to $t_{go,MT1}$ in $\boldsymbol{A}(t)$ (see Appendix A) and $\boldsymbol{A}(t)$ becomes singular when $t_{go,MM} = \Delta$.

In this work, we use the classical linearized method to approximate $t_{go,E}$ of the collision geometry E, $E \in \{MT1, MT2, MM\}$, at each time step. Let $t_{go,E}^{lin}$ be the linear approximation for the $t_{go,E}$, then

$$t_{go,E}^{lin} = \rho_E / V_{C,E}, \quad E \in \{MT1, MT2, MM\} \tag{34}$$

This method of estimating $t_{go,E}^{lin}$ can deviate far from the true value especially when there are large changes to the initial collision geometry. Depending on initial conditions, such errors in $t_{go,E}^{lin}$ could violate the condition in (12) although actual values of $t_{go,E}$ do not. Therefore, for the implementation of the SDRE-based controller in this paper, to avoid the aforementioned singularity issue, $\bar{t}_{go,MM}$ is used to approximate $t_{go,MM}$, where $\bar{t}_{go,MM}$ is defined by the following conditional statement:

Condition 1 *If* $t_{go,MM}^{lin} \neq \min(t_{go,MT1}^{lin}, t_{go,MT2}^{lin}, t_{go,MM}^{lin})$, *then*

$$\bar{t}_{go,MM} = \min(t_{go,MT1}^{lin}, t_{go,MT2}^{lin}) \tag{35}$$

else

$$\bar{t}_{go,MM} = t_{go,MM}^{lin} \tag{36}$$

While (35) clearly does not accurately depict the true kinematics of the problem, it is a heuristic method that allows us to avoid the singularity problem. It also makes physical sense to assume that the missile-missile collision, if it succeeds, should occur no later than earliest missile-target collision. Note while more accurate methods of approximating time-to-go exists in open literature (e.g., in [25]) the method proposed using Condition 1 is much simpler to implement and, as shown in the simulation results in Section V, proved to be sufficient for the implementation of the cooperative guidance law.

IV. Multiple-Model Adaptive-Control-Based Cooperative Guidance Law

In order for the target pair to maneuver optimally against the pursuing missiles and lure them into collision, the targets are assumed to know exactly what guidance laws the missile team is using. In this section, an MMAE approach is proposed to identify the guidance laws

employed by the missile team, the relative states of the engagement, as well as the various time-to-go values necessary for the computation of the cooperative guidance strategy. The section begins with a brief review of the fundamental principles of MMAE before presenting the implementation of the estimator together with guidance law described in Section III under a MMAC framework.

IV.A. Multiple-Model Adaptive Estimator

The MMAE approach [14–16, 26, 27] is a well-established method of estimating unknown system parameters. The system is assumed to have a known finite set of possible regimes and the true regime is fixed. Filters are run in parallel and each filter matches one of the possible regimes (see for instance [14]).

In this work, it is assumed that the pursuing missiles are employing one of the p possible missile guidance strategies in the set $\mathcal{U}_i$, $i \in \{1, 2\}$, i.e.,

$$u_{Mi} \in \mathcal{U}_i \triangleq \{u_{Mi}^1, ..., u_{Mi}^j, ..., u_{Mi}^p\} \tag{37}$$

In addition, we assume in this paper that the target pair has perfect information on its own parameters associated to the estimation process ($\boldsymbol{x}_{Ti}$, γ_{Ti}, and V_{Ti}, $i \in \{1, 2\}$). It is also assumed that the target pair has exact information on the missile dynamics (for methods to identify the latter, readers are directed to [14, 15]). The estimation process is assumed to be decoupled between the two targets and the estimator of each target need only the measurements acquired by itself. Therefore, the jth regime dynamics is defined by the EOM presented in (3) with $u_{Mi} = u_{Mi}^j$ and can be compactly written in discrete time as:

$$\boldsymbol{x}_{MTi}^j(k) = \boldsymbol{f}_{k-1}^j\big(\boldsymbol{x}_{MTi}^j(k-1), \boldsymbol{u}_T(k-1)\big), \quad i \in \{1, 2\} \tag{38}$$

where $\boldsymbol{x}_{MTi}^j(k)$ is the discretized version of the state vector $\boldsymbol{x}_{MTi}(t_k)$ in (1) associated with the jth regime and $t_k = kT_s$, T_s is the sampling period used for estimation. The vector function $\boldsymbol{f}_{k-1}^j$ is obtained by integrating the EOMs of the jth regime from t_{k-1} to t_k. In this work, EKF matching the regime dynamics is used to calculate the time update state estimate since the engagement kinematics is nonlinear.

Next, using Bayes' rule, the jth regime probability at the kth time step, $\mu_i^j(k)$, can be determined by the following recursive formula [26], based on a given initial probability, $\mu_i^j(0)$:

$$\mu_i^j(k) = \frac{\Lambda_i^j(k)\mu_i^j(k-1)}{\sum_{l=1}^p \Lambda_i^j(k)\mu_i^j(k-1)}, \quad j \in \{1, ..., p\} \tag{39}$$

where $\Lambda_i^j(k) \triangleq f_p(\boldsymbol{z}_i(k)|\boldsymbol{z}_i(1:k-1), u_{Mi}^j)$ is the jth regime-conditioned likelihood function

computed based on the innovations process statistics of the jth filter of the ith missile, $\boldsymbol{z}_i(1:k)$ is the measurement acquired by the ith missile from 1st time step to the kth, and $f_p(\mathcal{A}|\mathcal{B})$ is the conditional probability density function of $\mathcal{A}$ given $\mathcal{B}$.

Under linear-Gaussian assumptions, $\Lambda_i^j(k)$ is also Gaussian and is thus

$$\Lambda_i^j(k) = \mathcal{N}(\boldsymbol{\nu}_i^j(k); [0]_{n_z \times 1}, \boldsymbol{S}_i^j(k)) \tag{40}$$

where $\boldsymbol{\nu}_i^j(k)$ and $\boldsymbol{S}_i^j(k)$ are the innovation and its covariance from the jth regime-matched filter.

IV.B. MMAE for Identification of Classical Guidance Laws

In this work, the cooperative targets guidance law is derived against a missile team using the well-established classical guidance laws PN, APN and OGL. Application of these guidance laws is usually in its nonlinear form rather than the linearized formulation presented in (24). For the sake of brevity, the index for the ith missile or target, $i \in \{1, 2\}$ is dropped in the formulation of this subsection:

$$u_M^j = N'_{GL} \frac{Z_{GL}}{t_{go,MT}^2 \cos(\gamma_M - \lambda_{MT})} \qquad GL \in \{PN, APN, OGL\} \tag{41}$$

where N'_{GL} is the effective navigation gain, Z_{GL} is the missile's ZEM distance, which is unique for each guidance law:

$$Z_{PN} = V_{C,MT} \dot{\lambda}_{MT} t_{go,MT}^2 \tag{42a}$$

$$Z_{APN} = Z_{PN} + \frac{t_{go,MT}^2}{2} a_T^{\perp} \tag{42b}$$

$$Z_{OGL} = Z_{APN} - a_M^{\perp} \tau_M^2 \psi(\xi_{MT}) \tag{42c}$$

where $\dot{\lambda}_{MT}$ and $V_{C,MT}$ are defined in (3) and (4) respectively. Variables $a_T^{\perp}$ and $a_M^{\perp}$ are the components of the target and missile accelerations orthogonal to the missile-target LOS as presented in (20) and (21). And $\psi(\xi)$ is defined as

$$\psi(\xi_{MT}) = \exp(-\xi_{MT}) + \xi_{MT} - 1 \tag{43}$$

where $\xi_{MT} \triangleq t_{go,MT}/\tau_M$ is the non-dimensionalized time-to-go.

While N'_{GL} are constants for PN and APN, N'_{OGL} is a function of ξ_{MT} and is defined as:

$$N'_{OGL} = \frac{6\xi_{MT}^2\psi(\xi_{MT})}{3 + 6\xi_{MT} - 6\xi_{MT}^2 + 2\xi_{MT}^3 - 3\exp(-2\xi_{MT}) - 12\xi_{MT}\exp(-\xi_{MT})} \tag{44}$$

Thus to determine the guidance law of the missiles, the MMAE is required to identify the ZEM values, (42), and in the case of PN and APN, N'_{GL}.

IV.C. Estimating the Range and Line-of-Sight Angle Between M1 and M2

Besides the states associated with the missile-target collision geometries, the cooperative guidance law defined in Section III requires also the states ρ_{MM} and λ_{MM} for computation of the linearized states. In this work, these states are computed separately out of the estimation loop using the estimates of ρ_{MTi} and λ_{MTi}, $i \in \{1, 2\}$ and the relative position of the targets. This way estimation can be decoupled between the targets and they need only compute the number of filters that corresponds to the p number of possible guidance laws.

Let ρ_{TT} and λ_{TT} (see Figure 2) define the relative position between the targets in polar coordinates and assuming we have perfect information on these parameters. Then by taking reference from one of the targets, say $T1$, ρ_{MM} and λ_{MM} can be computed:

$$\left.\begin{aligned} \rho_{MM} &= \sqrt{\Delta X_{MM}^2 + \Delta Y_{MM}^2} \\ \lambda_{MM} &= \arctan(\Delta Y_{MM}/\Delta X_{MM}) \end{aligned}\right\} \tag{45}$$

where

$$\Delta X_{MM} = \rho_{TT}\cos\lambda_{TT} - \rho_{MT2}\cos\lambda_{MT2} + \rho_{MT1}\cos\lambda_{MT1} \tag{46}$$

$$\Delta Y_{MM} = \rho_{TT}\sin\lambda_{TT} - \rho_{MT2}\sin\lambda_{MT2} + \rho_{MT1}\sin\lambda_{MT1} \tag{47}$$

Estimates $\hat{\rho}_{MM}$ and $\hat{\lambda}_{MM}$ can then be computed using equations (45) to (47) based on the estimates $\hat{\rho}_{MT1}$, $\hat{\rho}_{MT2}$, $\hat{\lambda}_{MT1}$, $\hat{\rho}_{MT2}$, and variables ρ_{TT} and λ_{TT} in which we assumed to have perfect information of.

Remark 2 *If the estimation process is coupled between $T1$ and $T2$, i.e., ρ_{MM} and λ_{MM} are estimated by incorporating their dynamics* (7) *into the EKF equations, then the number of filters increases drastically with p since in addition to the number of possible guidance laws employed by each missile, the MMAE scheme has to compute p^2 number of filters in parallel to account for the possible combinations of guidance laws employed by the 2 missiles. Also, the size of the covariance matrix to be solved by each filter increases from 5×5 (5 states for each $Mi - Ti$ engagement, $i \in \{1, 2\}$) to 12×12 (10 states for both $Mi - Ti$ engagements plus ρ_{MM} and λ_{MM}). This can become very computationally intensive with increasing p.*

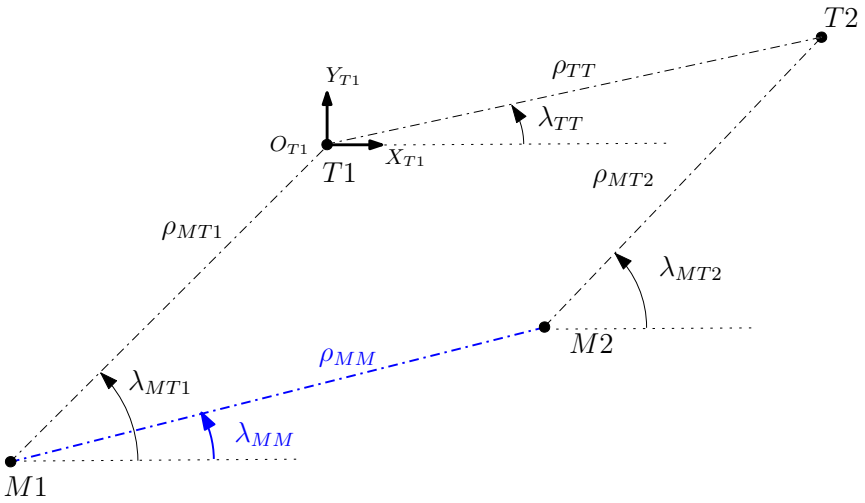

Figure 2: Relative positions of $M1$ & $M2$ referenced to $T1$.

IV.D. MMAC-based Cooperative Guidance Law

In order to compute the maneuver commands for the target pair when information on the missiles is imperfect, this paper employs the MMAC approach [17]. In this approach, the state estimates from each filter are fed into a regime matched controller. The final target commands can then be computed by either: 1) minimum mean square error (MMSE), or 2) maximum a posteriori probability (MAP) approach.

IV.D.1. MMSE Approach

In the MMSE approach, the final target command $\boldsymbol{u}_T$ is determined by a weighted average of the regime-matched target commands. However, each regime-matched controller varies with different combinations of guidance laws used by the missile team, and in order to compute the final target commands using the MMSE approach would require multiple solutions of the Riccati equation (32) each accounting for every possible combination.

Consider each target, Ti, computes p number of regimes that corresponds to the list of possible guidance laws employed by its pursuer, Mi. Let $\mathcal{U}_{comb}$ denote the set that consists of all possible combinations of guidance laws between $M1$ and $M2$ and $\boldsymbol{u}_M^l$ the lth combination in this set, i.e.,

$$\boldsymbol{u}_M^l = \left[u_{M1}^{j1}, \quad u_{M2}^{j2}\right], \quad l \in \{1, ..., p^2\}, \quad j1, j2 \in \{1, ..., p\}, \quad \text{and} \quad \boldsymbol{u}_M^l \in \mathcal{U}_{comb} \tag{48}$$

If $\mathcal{U}_{comb}$ is arranged in the following order:

$$\mathcal{U}_{comb} \triangleq \left\{ \begin{array}{cccccccc} \boldsymbol{u}_M^1 & \triangleq & \left[u_{M1}^1, & u_{M2}^1\right]^T, & \cdots & , \boldsymbol{u}_M^p & \triangleq & \left[u_{M1}^1, & u_{M2}^p\right]^T \\ \boldsymbol{u}_M^{p+1} & \triangleq & \left[u_{M1}^2, & u_{M2}^1\right]^T, & \cdots & , \boldsymbol{u}_M^{2p} & \triangleq & \left[u_{M1}^2, & u_{M2}^p\right]^T \\ & & & & \vdots & & & & \\ \boldsymbol{u}_M^{(p-1)p+1} & \triangleq & \left[u_{M1}^p, & u_{M2}^1\right]^T & \cdots & , \boldsymbol{u}_M^{p^2} & \triangleq & \left[u_{M1}^p, & u_{M2}^p\right]^T \end{array} \right\} \tag{49}$$

then the index l can be written as a function of $j1$ and $j2$,

$$l = (j1 - 1)p + j2 \tag{50}$$

The combined regime probability of $\boldsymbol{u}_M^l$ at time step k, $\mu^l(k)$, is calculated based on the regime probabilities associated with the $j1$-th and $j2$-th regimes in the MMAE of $T1$ and $T2$, i.e.,

$$\mu^l(k) = \mu_1^{j1}(k)\mu_2^{j2}(k), \quad l \in \{1, ..., p^2\} \tag{51}$$

The final command at time step k in a MMSE sense is,

$$\boldsymbol{u}_T^{(mmse)} = \sum_{l=1}^{p^2} \mu^l(k)\boldsymbol{u}_T^{*l}, \tag{52}$$

where $\boldsymbol{u}_T^{*l} = \left[u_{T1}^{*l}, \quad u_{T2}^{*l}\right]^T$, $l \in \{1, ..., p^2\}$ is the optimal maneuver based on the cooperative guidance strategy as formulated in Section III against the lth combination of missile guidance laws.

Remark 3 *If the estimation is coupled, then both MMAE scheme and Riccati equation* (32) *will be computed* p^2 *number of times in parallel. Instead of* (51)*,* $\mu^l(k)$ *will simply correspond to regime probability of the* l*th regime in the* p^2 *number of filters in the coupled MMAE scheme.*

IV.D.2. MAP Approach

In the MAP approach, $\boldsymbol{u}_T$ is determined as the command against the combination of missile guidance laws that has the maximum a posteriori probability. In this approach, only one solution to (32) is required since we only need to compute the SDRE controller for the combination of guidance laws that corresponds to the regimes with the highest probability

from each target's MMAE. Consider the following:

$$\left.\begin{aligned} j1 &= \arg \max_{j\in\{1,\dots,p\}} \mu_1^j(k) \\ j2 &= \arg \max_{j\in\{1,\dots,p\}} \mu_2^j(k) \end{aligned}\right\} \tag{53}$$

then

$$\boldsymbol{u}_T^{(map)} = \boldsymbol{u}_T^{*l} \tag{54}$$

where l relates to indices $j1$ and $j2$ through (50), and it is the index in $\mathcal{U}_{comb}$ as defined by (49).

Remark 4 *If the estimation process is coupled, then a total of p^2 number of filters need to be run in parallel. However, unlike in MMSE approach, $\boldsymbol{u}_T^{(map)}$ only needs* (32) *to be solved once at each time step for $\boldsymbol{u}_T^{*l}$ instead of solving all p^2 number of regime-matched optimal maneuvers as shown in* (52)*.*

IV.E. Sensitivity of Guidance Law to Estimation Performance

The cooperative guidance law derived in Section III follows a similar geometric rule to the classical PN in which collision is achieved if the associated vehicles are able to remain on the collision triangle. The targets must therefore ensure that the LOS rate between the missiles are nullified towards the end of the engagement. Hence, accuracy of the estimate for the LOS angle between the missiles, λ_{MM}, becomes paramount to achieving good miss-distance performance. Figure 3 depicts the effects of missile-target estimation errors on the estimation error of λ_{MM}. Here, the accent "˜" denotes the estimation error of the associated parameter. For the purpose of this discussion, it is assumed that states of $M1$ are known perfectly and $\tilde{\lambda}_{MM}$ is attributed to errors in state estimates of the $M2-T2$ engagement. We introduce another parameter in this discussion, $\tilde{y}_{MM}$, which represents the difference in the true and estimated position of $M2$. The parameter $\tilde{y}_{MM}$ can also be viewed as the miss-distance associated with estimation error, $\tilde{\lambda}_{MM}$. Assuming estimation errors are small near the end of $M1-M2$ engagement, using small angle approximations, $\tilde{y}_{MM}$, can be written as:

$$\tilde{y}_{MM} \simeq \rho_{MM}\tilde{\lambda}_{MM} = \sqrt{\tilde{y}_{MT2}^2 + \tilde{\rho}_{MT2}^2} \tag{55}$$

such that

$$\tilde{y}_{MT2} \simeq \rho_{MT2}\tilde{\lambda}_{MT2} \tag{56}$$

From (55) and (56), it is clear that contribution of $\tilde{\lambda}_{MT2}$ to $\tilde{y}_{MM}$ diminishes as the range between the $M2$ and $T2$ decreases. Assuming $\tilde{\lambda}_{MT2}$ and $\tilde{\rho}_{MT2}$ converges to its asymptotic value towards the end of the engagement and $\dot{\rho}_{MT2} < 0$, the influence of $\tilde{\lambda}_{MT2}$ on $\tilde{y}_{MM}$ reduces as compared to $\tilde{\rho}_{MT2}$ as the missile approaches the target. Thus, the quality of the range estimate between the missile and the target becomes the dominant factor influencing the cooperative guidance law's miss distance performance.

To have some quantitative assessment on the influence of errors in range and LOS angle estimates between the missiles and targets towards $\tilde{y}_{MM}$, we compute and tabulate $\tilde{y}_{MM}$ in Table 1 using Eq. (55) for various error levels in the missile-target state estimates for the case when $\hat{\rho}_{MT2} = 2000$ m at $t_{f,MM}$. Here it is assumed that the missiles have a non-zero miss (i.e., $\rho_{MM} \neq 0$) at $t_{f,MM}$.

Case	$\tilde{\lambda}_{MT2}$ [mrad]	$\tilde{\rho}_{MT2}$ [m]	$\tilde{y}_{MT2}$ [m]	$\tilde{y}_{MM}$ [m]
Nominal	0.25	1.5	0.5	1.581
$0.1 \times \tilde{\lambda}_{MT2}$	0.025	1.5	0.05	1.501
$0.1 \times \tilde{\rho}_{MT2}$	0.25	0.15	0.5	0.522

Table 1: Missile–missile miss distance due to estimation errors from missile–target engagement

As seen in Table 1, a significant reduction in $\tilde{y}_{MM}$ is achieved for a given ρ_{MM} only in the case when $\tilde{\rho}_{MT2}$ is reduced. This influence of the range estimation accuracy between the missile-target on $\tilde{y}_{MM}$ will be further validated in the Monte Carlo studies in Section V.B.3.

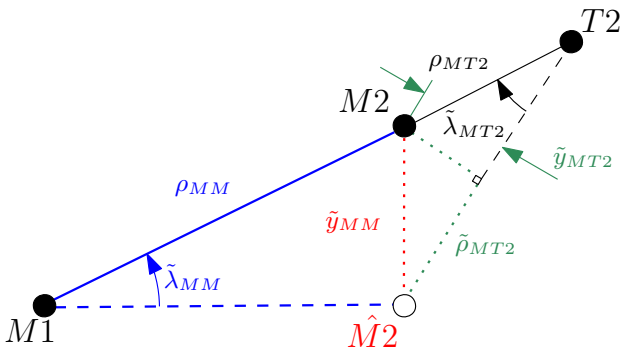

Figure 3: Effects of missile-target estimation errors on missile-missile miss-distance estimation, $\tilde{y}_{MM}$.

V. Simulation Analysis

In this section, the performance of the cooperative target guidance strategy derived in Section II is presented. The section begins by evaluating the proposed guidance law using perfect information, where we demonstrate the importance of the weights on δ_{MM} and θ_{MM}

in the cost function (28). A "collision map" is presented thereafter in which the ability of the target team to lure the missile into collision based on different initial conditions is shown.

In the subsequent subsection, performance of the guidance law using the estimated states (i.e., "estimation-in-the-loop") is analyzed in Monte Carlo (MC) simulations. Results from a sample run are also presented in this subsection to demonstrate the performance of the estimator. Sensitivity of the cumulative distribution function (CDF) of the missile-missile miss distance to measurement noise is also evaluated.

V.A. Guidance Law Performance with Perfect Information

V.A.1. Simulation Setup

The simulation setup is as follows. All vehicles have constant speeds: $V_{M1} = V_{M2} = 600\ m/s$, $V_{T1} = V_{T2} = 400\ m/s$. Flight path angles were set such that $\gamma_{T1} = \gamma_{T2} = 0^\circ$ and missiles have zero initial heading error. The guidance laws for $M1$ and $M2$ are APN, with $N'_{APN} = 5$, and OGL respectively. All vehicles have 1st-order dynamics with time lag constants, $\tau_M = 0.25\ s$ for both missiles and $\tau_T = 0.5\ s$ for both targets. Accelerations were bounded at $a_T^{max} = 10$ g for both targets and at $a_M^{max} = 20$ g for both missiles where g $= 9.80665\ m/s^2$ is the gravitational constant. Control update frequency is set at 50 Hz. Unless otherwise stated, weights on the cost function (28) are set as such: $w_{ms} = 1e4$, $w_{u1} = w_{u2} = 0.003$ and $w_\delta = w_\theta = 30$.

V.A.2. Influence of Weights on Guidance Performance

In this subsection, the weights on δ_{MM} and θ_{MM} from the cost function (28), w_δ and w_θ respectively, are varied to demonstrate its influence on the guidance performance. Referring to Figure 4, when $w_\delta = w_\theta = 0$, the targets simply maneuver to minimize the change in LOS between the missiles (through minimizing $y_{MM}(t_{f,MM})$ in the linear system). While the targets were able to guide the missiles to be on a collision course, they were not able to do so before $M2$ collided with $T2$. When $w_\delta = w_\theta = 30$, the targets maneuver to reduce δ_{MM} and θ_{MM}, thus driving the missiles to collide at an earlier time. It is important to note that the weights were tuned to ensure zero miss between the missiles: values too high compared to the weight on $y_{MM}(t_{f,MM})$ will result in non-zero miss while values too low (similar to $w_\delta = w_\theta = 0$) lead to collision between missile(s) and target(s).

Remark 5 *In the proposed guidance law, collision avoidance between the targets is not explicitly accounted for. Thus, in the singular cases, e.g., when the engagement has perfect symmetry (i.e., in position, target/missile velocities, missile guidance laws), the targets may collide before the missiles do. In order to avoid target-target collision, the target pair can 1)*

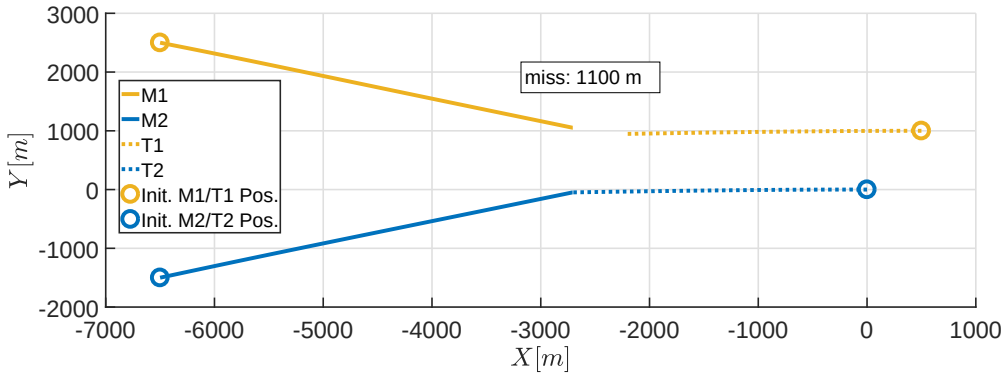

(a) $w_\delta = w_\theta = 0$

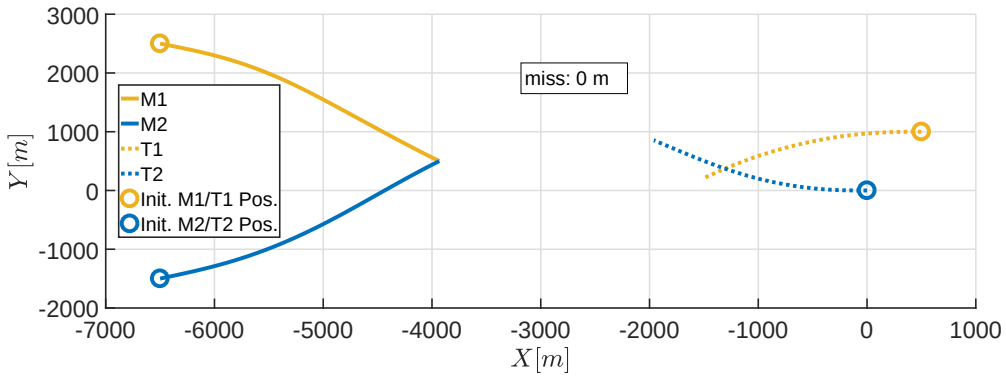

(b) $w_\delta = w_\theta = 30$

Figure 4: Influence of the weights on the relative angles between missiles' heading and the LOS between them.

fly in an asymmetric formation as shown in Figure 4*, 2) fly at different velocities and/ or 3) implement an anti-collision guidance strategy.*

V.A.3. Collision Map

The performance of the guidance law is evaluated over a range of initial conditions and presented in a "collision map". Missile and target parameters are the same as described in Section V.A.1. Target positions are fixed at the same location as seen in Figure 4 while positions of the missiles are varied.

Positions of the missiles are varied as follows. Referring to Figure 5, the missiles' initial LOS angle is fixed at $\lambda^0_{MM} = -\pi/2$ (i.e., parallel to the Y_I axis). The center of missile-missile LOS is denoted as c and the initial inertial position of c is (X^0_c, Y^0_c). The initial range between the missiles ρ^0_{MM}, together with X^0_c and Y^0_c are varied over the intervals $\rho^0_{MM} \in [100, 6000]$ m, $X^0_c \in [-10000, -1000]$ m, and $Y^0_c \in [-3000, 3000]$ m. These parameters are normalized

by the initial range between the targets, ρ_{TT}^0 and are denoted as $\bar{\rho}_{MM}^0$, $\bar{X}_c^0$ and $\bar{Y}_c^0$, i.e.,

$$\bar{\rho}_{MM}^0 \triangleq \rho_{MM}^0/\rho_{TT}^0, \qquad \bar{X}_c^0 \triangleq X_c^0/\rho_{TT}^0, \qquad \bar{Y}_c^0 \triangleq Y_c^0/\rho_{TT}^0 \tag{57}$$

The collision maps obtained from the simulations are presented in Figure 6 in which initial conditions that resulted in missile-missile collision are marked with circles while conditions which led to a miss are marked by asterisks. Missiles are considered to have "collided" if $\rho_{MM}(t_{f,MM}) \leq 0.1$ m.

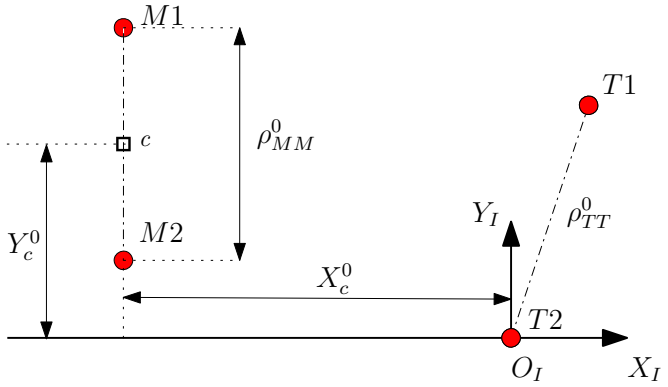

Figure 5: Relative positions of $M1$ & $M2$ referenced to $T1$.

As shown in Figure 6, the guidance law is most effective when $\bar{\rho}_{MM}^0 > 1$, $\bar{X}_c^0$ is large and when $\bar{Y}_c^0$ is small. This is intuitive as observed in the sample trajectory in Figure 4, the targets require sufficient initial separation between themselves and the missiles so that the target pair has sufficient time to lure the pursuers into collision. The guidance is less effective when $\bar{\rho}_{MM}^0 < 1$, i.e $\rho_{MM}^0 < \rho_{TT}^0$. In such scenarios, the missile velocities are initially pointing away from each other (since we assumed that the missiles have zero initial heading error) and with decreasing $\bar{X}_c^0$, the initial difference between the missile headings becomes too large for the target pair to turn the missiles into head-on collision before one of the targets is intercepted. Also, as seen in Figures 6c and 6d, the targets were able to enforce collision if $\bar{Y}_c^0 \sim [-1, 2]$. This is also intuitive since a large offset in the center point c meant that one of the missile is closer to the target than the other and target interception would occur earlier than the missile-missile collision.

V.B. Monte Carlo Study with "Estimator-in-the-loop"

V.B.1. Simulation Setup

A Monte Carlo study was conducted to evaluate the "estimator-in-the-loop" performance of the cooperative guidance law. Inertial positions are the same as that shown in Figure 4 and are fixed in this study. Initial flight path angles of the targets are uniformly selected

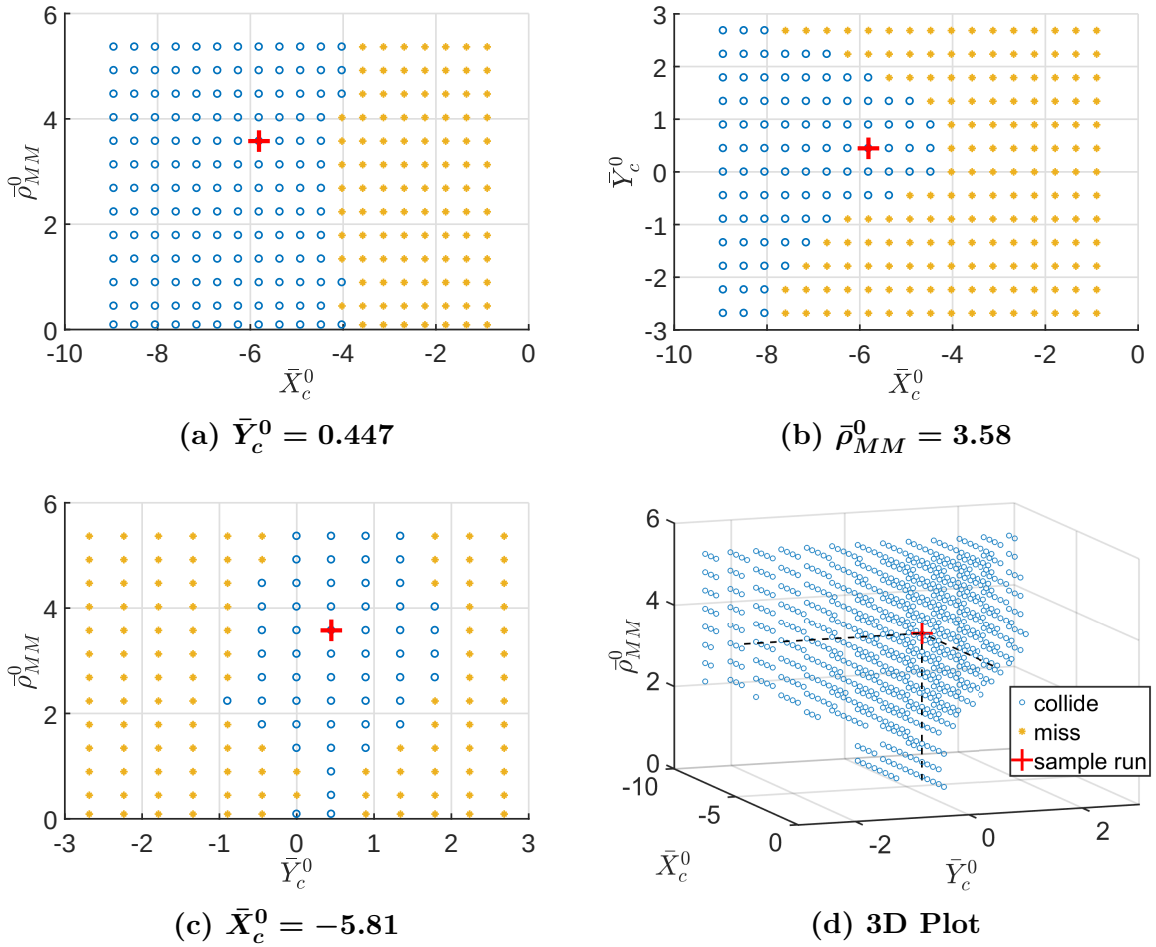

(a) $\bar{Y}_c^0 = 0.447$ **(b)** $\bar{\rho}_{MM}^0 = 3.58$

(c) $\bar{X}_c^0 = -5.81$ **(d) 3D Plot**

Figure 6: Collision map. Data points where a missile hits its target were excluded in (d) for clarity.

from the interval $[-10, 10]$ deg, whereas the initial heading errors of the missiles are drawn from a zero-mean normal distribution with 3° standard deviation. The guidance law that is employed by each missile is assumed to be one of the 7 regimes considered by each target in this study. This includes: PN, APN, and OGL with $N'_{GL} \in \{3, 4, 5\}$ for $GL \in \{\text{PN, APN}\}$. Selection of the missiles' guidance laws at the beginning of each run is based on the initial regime probability, $\mu_i^j(0)$, $i \in \{1, 2\}$, $j \in \{1, ..., 7\}$. $\mu_i^j(0)$ is set such that each type of guidance law has 1/3 probability and each N'_{GL} has a 1/9 chance of occurring within the guidance law. Each MC simulation includes 500 runs.

In this study, the MAP approach is employed for MMAC (see Section IV.D.2) as it is computationally more efficient and is more practical to implement on the on-board processor of an aircraft/missile. Each filter of the ith estimator is initiated with the same state estimate, $\hat{\boldsymbol{x}}^j_{MTi}(0|0) \sim \mathcal{N}(\boldsymbol{x}_{MTi}(0), \boldsymbol{P}(0|0))$, $i \in \{1, 2\}$, $j \in \{1, ..., 7\}$, where $\boldsymbol{x}_{MTi}(0)$ is the true initial state and the initial covariance $\boldsymbol{P}(0|0) = \text{diag}\{650^2, (3\pi/180)^2, (5\text{g})^2, (3\pi/180)^2, 60^2\}$.

The targets are assumed to be acquiring both range and bearing measurements that are corrupted by noises as defined in (11). Variances of the measurement noises are varied in this study to assess the sensitivity of the cooperative guidance law to noise. Measurements are taken at a frequency of 50 Hz.

V.B.2. Sample Run

A sample run is presented here to demonstrate the performance of the estimator and the guidance law when using imperfect information. In this sample run, $\sigma_\rho = 10\ m$ and $\sigma_\lambda = 1$ *mrad*. Missile and target parameters follow exactly as described in Section V.A.1.

Convergence of the regime probabilities μ_1^j and μ_2^j are shown in Figure 7. As seen in the figure, regime probabilities for both missiles converged to 1 by $t = 4\ s$. Convergence of μ_2^j is slower as the guidance behaviors for OGL and APN, $N'_{APN} = 3$ (i.e., the optimal guidance gain for APN) are very similar. They differ only in the term associated with the $M2$'s first order lag, τ_{M2} (see (42)), and since $\tau_{M2} = 0.25\ s$, contribution from this term is hardly discernible. While this is true, $T2$'s estimator correctly identified OGL as the most probable guidance law being employed by $M2$ throughout the engagement, and since it is using the MAP approach to derive its optimal maneuver, it is still behaving optimally against $M2$.

For brevity, only the estimation performance of the states relating to the $M2-T2$ and $M1-M2$ engagements are presented as similar results are seen in the $M1-T1$ case. Despite the slower convergence in the regime probabilities in $T2$'s estimator, the state estimation errors converges to their asymptotic values at around $2s$, as seen in Figure 8. Note that since $\hat{\rho}_{MM}$ and $\hat{\lambda}_{MM}$ are computed using (45) and not within the estimator, hence only the sample errors without the variances are shown in Figure 8. For other estimates presented in Figure 8, the error performance is obtained based on the blended estimate $\hat{\boldsymbol{x}}_{MTi}$ and blended covariance $\boldsymbol{P}_{MTi}$ and are calculated using:

$$\hat{\boldsymbol{x}}_{MTi}(k|k) = \sum_{j=1}^{p} \mu_i^j(k)\hat{\boldsymbol{x}}_{MTi}^j(k|k) \tag{58a}$$

$$\boldsymbol{P}_{MTi}(k|k) = \sum_{j=1}^{p} \mu_i^j(k)\left[\boldsymbol{P}_{MTi}^j(k|k) + \bar{\boldsymbol{P}}_{MTi}^j\right] \tag{58b}$$

where $\hat{\boldsymbol{x}}_{MTi}^j(k|k)$, $j \in \{1, ..., p\}$ and $\boldsymbol{P}_{MTi}^j(k|k)$ are the jth regime estimate and covariance of the ith estimator respectively and

$$\bar{\boldsymbol{P}}_{MTi}^j \triangleq \left[\hat{\boldsymbol{x}}_{MTi}^j(k|k) - \hat{\boldsymbol{x}}_{MTi}(k|k)\right]\left[\hat{\boldsymbol{x}}_{MTi}^j(k|k) - \hat{\boldsymbol{x}}_{MTi}(k|k)\right]^T \tag{59}$$

Engagement trajectories of the sample run are shown in Figure 9 and are very similar to what was depicted in Figure 4b. Missile-misile miss distance in this run was 0.599 m.

Acceleration profiles of the target pair in this sample run when using imperfect and perfect information (labeled a_{Ti}^{map} and a_{Ti}^{*} respectively, $i \in \{1, 2\}$) are plotted in Figure 10. Initial disparities between a_{Ti}^{map} and a_{Ti}^{*} are observed due to large estimation errors. As estimation errors converge at $t \sim 2$ s, a_{Ti}^{map} behaves close to that of a_{Ti}^{*}. The kink observed in a_{Ti}^{map} near $t = 5.4$ s was due to divergence of $\tilde{\lambda}_{MM}$ as observed in Figure 8. The divergence is consistent with what was derived in (55), as $\tilde{\lambda}_{MM}$ increases exponentially as ρ_{MM} approaches zero.

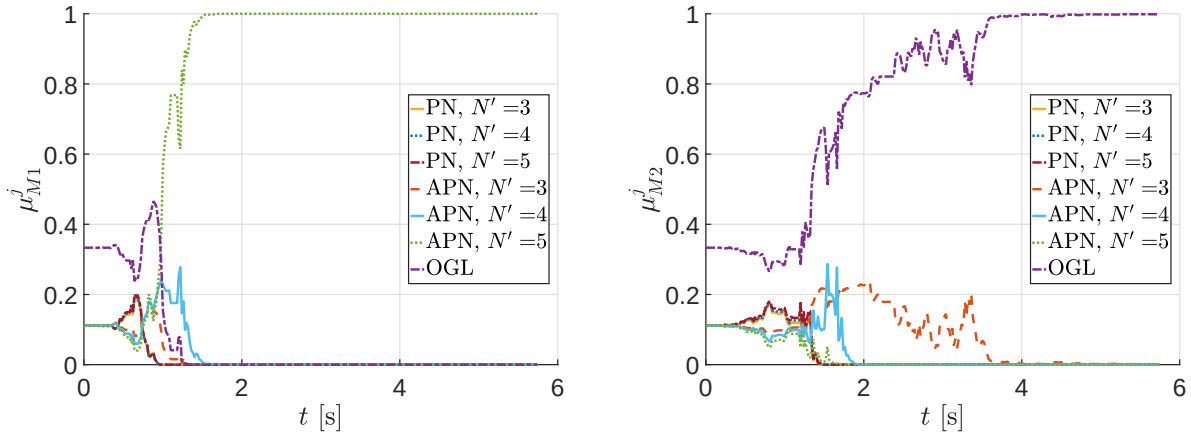

(a) $T1$ **(b) $T2$**

Figure 7: Regime probabilities of $T1$'s and $T2$'s estimator. $M1$ is using APN with $N'_{APN} = 5$ while $M2$ is using OGL.

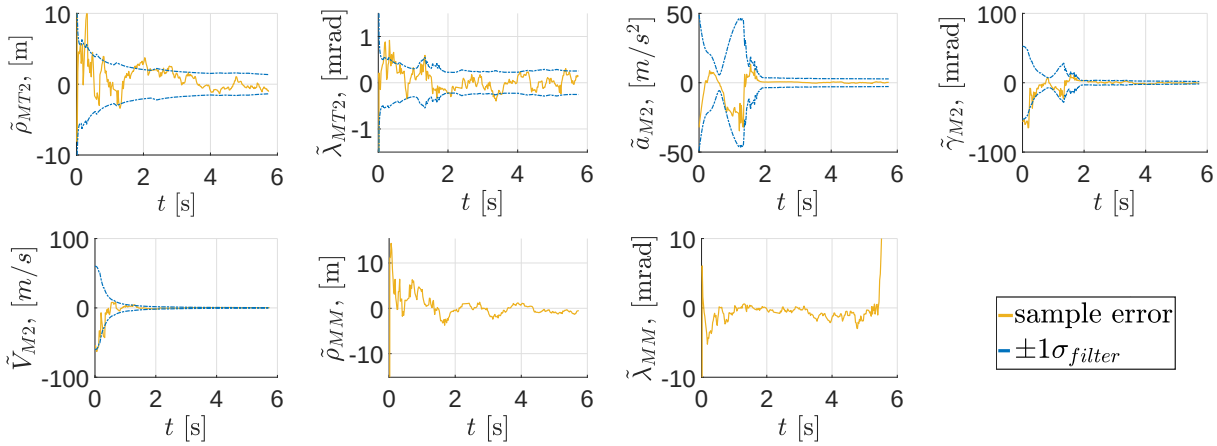

Figure 8: Sample estimation error performance.

V.B.3. Monte Carlo Study

Results of the MC simulations are presented in this subsection. The performance metric in this study is the CDF of the miss distance between the missiles. The sensitivity of the miss CDF to measurement noise is evaluated here. Measurement noise variances are the

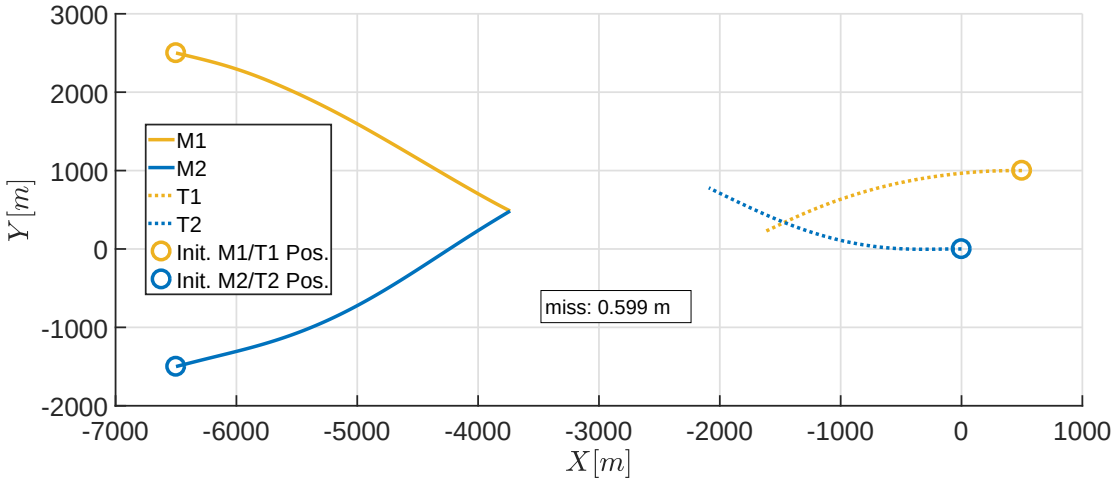

Figure 9: Engagement trajectories when targets are using MMAC with $M1$ using APN, $N'_{APN} = 5$, and $M2$ using OGL.

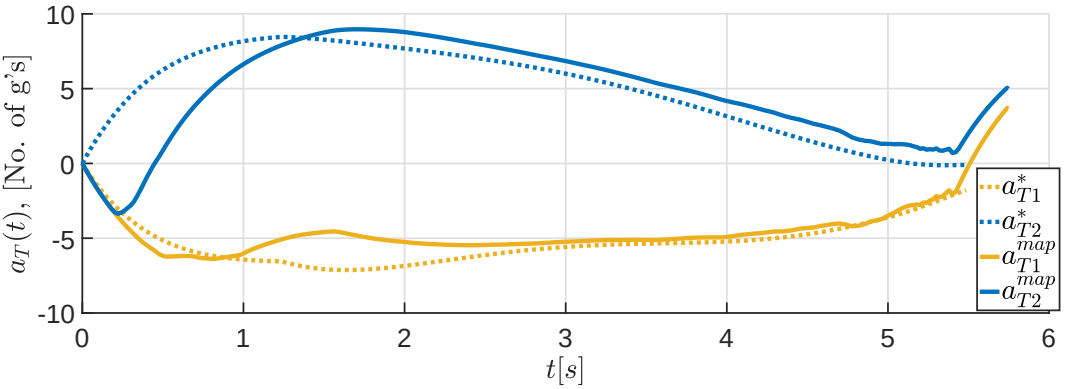

Figure 10: Target acceleration profiles.

same for both targets, i.e., $\sigma_{i,\rho} = \sigma_\rho$ and $\sigma_{i,\lambda} = \sigma_\lambda$, for $i \in \{1, 2\}$. Figure 11 shows the CDF of the missile-missile miss distance for different levels of noise in the range and bearing measurements. As shown in Figure 11, the miss CDF improves drastically with the reduction in σ_ρ. The results shown in Figure 11 substantiates the discussion in Section IV.E as the accuracy of the range estimates between the missile-target significantly affects the target pair's ability to accurately nullify the missile-missile LOS and keep the pursuers on their collision triangle.

VI. Conclusions

A novel optimal cooperative defensive strategy in a 2-on-2 engagement was derived in this paper. The proposed strategy capitalizes on the presence of multiple adversaries to lure them into collision. With the proposed MMAE scheme, the targets are able to identify the

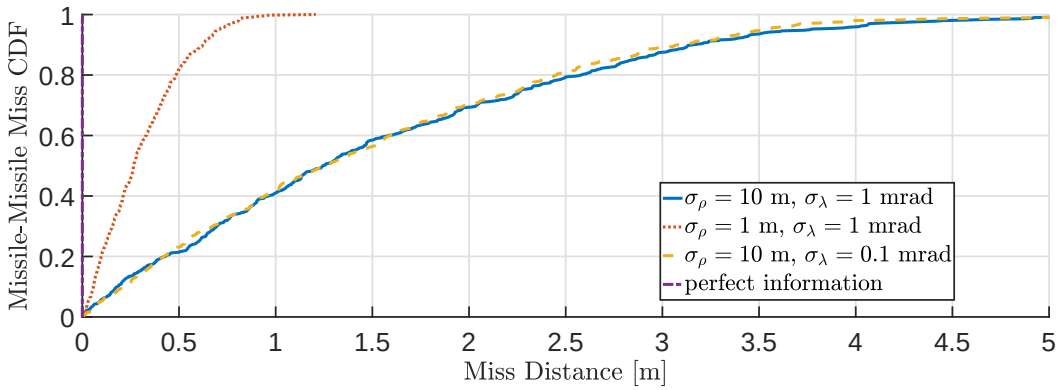

Figure 11: Sensitivity of missile-missile miss distance to measurement noise.

missiles' guidance laws and predict their future trajectories. This information allows the target pair to maneuver cooperatively and set their pursuers on a collision triangle such that the missiles will hit each other before they could reach any of their targets.

When using perfect information, the proposed guidance strategy was shown to be effective over a wide range of initial conditions, as demonstrated by the collision map. This is despite the fact that the targets had half the maximum allowable acceleration and double the time lag compared to the missiles. This result highlights the advantage of the proposed cooperative strategy over conventional defensive strategies such as evasion or deploying defenders as the target pair was able to survive the engagement despite being less agile and not carrying any defending missiles.

For the case when the targets use imperfect information, a decentralized MMAC scheme was presented. Unlike the conventional MMAE approach in which the number of required filters for guidance law identification grows quadratically with the number of possible missile guidance strategies, number of filters in the proposed decentralized scheme grows only linearly. Sensitivity of the proposed guidance law to the estimation error of the missile-target range was also presented analytically and the findings were verified by Monte Carlo simulations.

Finally, it is important to note that the effectiveness of the guidance law also depends on the appropriate tuning of the weights in the cost function. Therefore, its is critical for the designer to make adjustments to the weights, if necessary, based on the required engagement conditions when applying the proposed guidance law.

Acknowledgement

This effort was sponsored by the U.S. Air Force Office of Scientific Research, Air Force Materiel Command, under grant number FA9550-15-1-0429. The U.S. Government is autho-

rized to reproduce and distribute reprints for Governmental purpose notwithstanding any copyright notation thereon.

Appendix A: Definition of $\boldsymbol{A}(t)$ and $\boldsymbol{B}(t)$ in (27)

Referring to (27), the sub-matrices in $\boldsymbol{A}(t)$ are defined as follows. The sub-matrix $\boldsymbol{A}_{MTi}$ represents the influence of the ith missile on the $Mi-Ti$ engagement:

$$\boldsymbol{A}_{MTi}=\begin{bmatrix} 0 & 1 & [0] & [0] \\ -d_{Mi}K_1^{Mi} & -d_{Mi}K_2^{Mi} & -[\boldsymbol{C}_{Mi}+d_{Mi}\boldsymbol{K}_{Mi}] & \boldsymbol{C}_{Ti}-d_{Mi}\boldsymbol{K}_{Ti} \\ \boldsymbol{B}_{Mi}K_1^{Mi} & \boldsymbol{B}_{Mi}K_2^{Mi} & \boldsymbol{A}_{Mi}+\boldsymbol{B}_{Mi}\boldsymbol{K}_{Mi} & \boldsymbol{B}_{Mi}\boldsymbol{K}_{Ti} \\ [0] & [0] & [0] & \boldsymbol{A}_{Ti} \end{bmatrix}, \quad i\in\{1,2\}$$

while $\boldsymbol{A}_{MM}^{Mi}$ represents the influence of the ith missile on the $M1-M2$ collision geometry:

$$\boldsymbol{A}_{MM}^{M1}= \frac{1}{C_{MT1}^{\delta}}\begin{bmatrix} 0 & 0 & [0] & [0] \\ -C_{MM}^{\delta}d_{M1}K_1^{M1} & -C_{MM}^{\delta}d_{M1}K_2^{M1} & -C_{MM}^{\delta}[\boldsymbol{C}_{M1}+d_{M1}\boldsymbol{K}_{M1}] & -C_{MM}^{\delta}d_{M1}\boldsymbol{K}_{T1} \\ d_{M1}K_1^{M1}/V_{M1} & d_{M1}K_2^{M1}/V_{M1} & [\boldsymbol{C}_{M1}+d_{M1}\boldsymbol{K}_{M1}]/V_{M1} & d_{M1}\boldsymbol{K}_{T1}/V_{M1} \\ 0 & 0 & [0] & [0] \end{bmatrix},$$

$$\boldsymbol{A}_{MM}^{M2}= \frac{1}{C_{MT2}^{\delta}}\begin{bmatrix} 0 & 0 & [0] & [0] \\ -C_{MM}^{\theta}d_{M2}K_1^{M2} & -C_{MM}^{\theta}d_{M2}K_2^{M2} & -C_{MM}^{\theta}[\boldsymbol{C}_{M2}+d_{M2}\boldsymbol{K}_{M2}] & -C_{MM}^{\theta}d_{M2}\boldsymbol{K}_{T2} \\ 0 & 0 & [0] & [0] \\ -d_{M2}K_1^{M2}/V_{M2} & -d_{M2}K_2^{M2}/V_{M2} & -[\boldsymbol{C}_{M2}+d_{M2}\boldsymbol{K}_{M2}]/V_{M2} & -d_{M2}\boldsymbol{K}_{T2}/V_{M2} \end{bmatrix},$$

and $\boldsymbol{A}_{MM}^{0}$ is defined as

$$\boldsymbol{A}_{MM}^{0}=\begin{bmatrix} \boldsymbol{A}^{0} & [0] \\ \boldsymbol{\Lambda}_{MM} & [0] \end{bmatrix}$$

where $\boldsymbol{A}^0$

$$\boldsymbol{A}^0 = \begin{bmatrix} 0 & 1 \\ 0 & 0 \end{bmatrix}$$

and $\boldsymbol{\Lambda}_{MM}$ consist of terms associated with $\dot{\lambda}_{MM}$

$$\boldsymbol{\Lambda}_{MM} = \frac{1}{V_{C,MM} t_{go,MM}^2} \begin{bmatrix} -1 & -t_{go,MM} \\ 1 & t_{go,MM} \end{bmatrix}$$

Next, we define $\boldsymbol{B}(t)$. Sub-matrix $\boldsymbol{B}_{MTi}$ describes the influence of the ith target on the $Mi - Ti$ engagement,

$$\boldsymbol{B}_{MTi} = \begin{bmatrix} 0 & d_{Ti} - d_{Mi} K_{u_{Ti}} & K_{u_{Ti}} \boldsymbol{B}_{Mi}^T & \boldsymbol{B}_{Ti}^T \end{bmatrix}^T, \qquad i \in \{1, 2\}$$

and sub-matrices $\boldsymbol{B}_{MM}^{Ti}$, $i \in \{1, 2\}$, represent the influence of the ith target on the $M1 - M2$ collision geometry:

$$\boldsymbol{B}_{MM}^{T1} = \frac{1}{C_{MT1}^{\delta}} \begin{bmatrix} 0 & -C_{MM}^{\delta} d_{M1} K_{u_{T1}} & d_{M1} K_{u_{T1}} / V_{M1} & 0 \end{bmatrix}^T$$
$$\boldsymbol{B}_{MM}^{T2} = \frac{1}{C_{MT2}^{\delta}} \begin{bmatrix} 0 & -C_{MM}^{\theta} d_{M2} K_{u_{T2}} & 0 & -d_{M2} K_{u_{T2}} / V_{M2} \end{bmatrix}^T$$

References

[1] Nigam, N. and Kroo, I., "Control and Design of Multiple Unmanned Air Vehicles for a Persistent Surveillance Task," in "12th AIAA/ISSMO Multidisciplinary Analysis and Optimization Conference, Multidisciplinary Analysis Optimization Conferences," Victoria, British Columbia, Sept. 2008, doi:10.2514/6.2008-5913. AIAA-2008-5913.

[2] Ousingsawat, J. and Campbell, M. E., "Optimal Cooperative Reconnaissance Using Multiple Vehicles," *Journal of Guidance, Control, and Dynamics*, Vol. 30, No. 1, 2007, pp. 122–132, doi:10.2514/1.19147.

[3] Jeon, I.-S., Lee, J.-I., and Tahk, M.-J., "Homing Guidance Law for Cooperative Attack

of Multiple Missiles," *Journal of Guidance, Control, and Dynamics*, Vol. 33, No. 1, 2010, pp. 275–280, doi:10.2514/1.40136.

[4] Earl, M. G. and D'Andrea, R., "A decomposition approach to multi-vehicle cooperative control," *Robotics and Autonomous Systems*, Vol. 55, No. 4, 2007, pp. 276–291, doi: 10.1016/j.robot.2006.11.002.

[5] Isaacs, R., *Differential games*, John Wiley & Sons, New York, 1965. pp. 336–356.

[6] Ho, Y., Bryson, A., and Baron, S., "Differential games and optimal pursuit-evasion strategies," *IEEE Transactions on Automatic Control*, Vol. 10, No. 4, 1965, pp. 385–389, doi:10.1109/TAC.1965.1098197.

[7] Breakwell, J. V. and Merz, A. W., "Minimum required capture radius in a coplanar model of the aerial combat problem," *AIAA Journal*, Vol. 15, No. 8, 1977, pp. 1089–1094, doi:10.2514/3.7399.

[8] Battistini, S. and Shima, T., "Differential Games Missile Guidance with Bearings-Only Measurements," *IEEE Transactions on Aerospace and Electronic Systems*, Vol. 50, No. 4, 2014, pp. 2906–2915, doi:10.1109/TAES.2014.130366.

[9] Borg, D. A. and Julich, P. M., "Proportional navigation vs an optimally evading, constant-speed target in two dimensions," *Journal of Spacecraft and Rockets*, Vol. 7, No. 12, 1970, pp. 1454–1457, doi:10.2514/3.30190.

[10] Slater, G. L. and Wells, W., "Optimal evasive tactics against a proportional navigation missile with time delay," *Journal of Spacecraft and Rockets*, Vol. 10, No. 5, 1973, pp. 309–313, doi:10.2514/3.27759.

[11] Shinar, J. and Steinberg, D., "Analysis of Optimal Evasive Maneuvers Based on a Linearized Two-Dimensional Kinematic Model," *Journal of Aircraft*, Vol. 14, No. 8, 1977, pp. 795–802, doi:10.2514/3.58855.

[12] Ben-Asher, J. Z. and Cliff, E. M., "Optimal evasion against a proportionally guided pursuer," *Journal of Guidance, Control, and Dynamics*, Vol. 12, No. 4, 1989, pp. 598–600, doi:10.2514/3.20450.

[13] Shima, T., "Optimal Cooperative Pursuit and Evasion Strategies Against a Homing Missile," *Journal of Guidance, Control, and Dynamics*, Vol. 34, No. 2, 2011, pp. 414–425, doi:10.2514/1.51765.

[14] Shaferman, V. and Shima, T., "Cooperative Multiple-Model Adaptive Guidance for an Aircraft Defending Missile," *Journal of Guidance, Control, and Dynamics*, Vol. 33, No. 6, 2010, pp. 1801–1813, doi:10.2514/6.2010-8320.

[15] Fonod, R. and Shima, T., "Multiple Model Adaptive Evasion Against a Homing Missile," *Journal of Guidance, Control, and Dynamics*, Vol. 39, No. 7, 2016, pp. 1578–1592, doi:10.2514/1.G000404.

[16] Magill, D., "Optimal adaptive estimation of sampled stochastic processes," *IEEE Transactions on Automatic Control*, Vol. 10, No. 4, 1965, pp. 434–439, doi:10.1109/TAC.1965.1098191.

[17] Lainiotis, D. G., "Partitioning: A unifying framework for adaptive systems, II: Control," *Proceedings of the IEEE*, Vol. 64, No. 8, 1976, pp. 1182–1198, doi:10.1109/PROC.1976.10289.

[18] Ratnoo, A. and Shima, T., "Line-of-Sight Interceptor Guidance for Defending an Aircraft," *Journal of Guidance, Control, and Dynamics*, Vol. 34, No. 2, 2011, pp. 522–532, doi:10.2514/1.50572.

[19] Kumar, S. R. and Shima, T., "Cooperative Nonlinear Guidance Strategies for Aircraft Defense," *Journal of Guidance, Control, and Dynamics*, Vol. 40, No. 1, 2017, pp. 124–138, doi:10.2514/1.G000659.

[20] Zarchan, P., *Tactical and strategic missile guidance*, American Institute of Aeronautics and Astronautics, Reston, VA, 2012, doi:10.2514/4.868948. Chap. 2.

[21] Garber, V., "Optimum intercept laws for accelerating targets," *AIAA Journal*, Vol. 6, No. 11, 1968, pp. 2196–2198, doi:10.2514/1.51611.

[22] Cottrell, R. G., "Optimal intercept guidance for short-range tactical missiles," *AIAA Journal*, Vol. 9, No. 7, 1971, pp. 1414–1415, doi:10.2514/3.6369.

[23] Bryson, A. and Ho, Y., *Applied optimal control: optimization, estimation and control*, Taylor & Francis Group, New York, 1975. pp. 146–152.

[24] Friedland, B., *Advanced Control System Design*, Prentice-Hall, Saddle River, NJ, 1996. pp. 110–112.

[25] Tahk, M.-J., Ryoo, C.-K., and Cho, H., "Recursive time-to-go estimation for homing guidance missiles," *IEEE Transactions on Aerospace and Electronic Systems*, Vol. 38, No. 1, 2002, pp. 13–24, doi:10.1109/7.993225.

[26] Bar-Shalom, Y. and Li, X.-R., *Estimation with Applications to Tracking and Navigation*, John Wiley & Sons, Inc., New York, 2001. Chap. 11.

[27] Oshman, Y., Shinar, J., and Weizman, S. A., "Using a Multiple-Model Adaptive Estimator in a Random Evasion Missile/Aircraft Encounter," *Journal of Guidance, Control, and Dynamics*, Vol. 24, No. 6, 2001, pp. 1176–1186, doi:10.2514/2.4833.